Seasonal ground deformation monitoring over Southern Larissa Plain (Central Greece) by SAR interferometry

I. Parcharidis, M. Foumelis, P. Katsafados

Department of Geography, Harokopio University of Athens, Athens, GR 176 71, Greece, parchar@hua.gr, mfoumelis@hua.gr, pkatsaf@hua.gr

Abstract Increase of water demand in Larissa Plain due to extensive cultivation, fulfilled by the over-exploitation of ground-water resource, lead to an intensive subsidence phenomenon causing in turns considerable damages to many buildings. DInSAR technique was proven to be a useful tool to measure ground deformation despite the unfavorable conditions inducing decorrelation. By exploiting differential interferometric pairs of short temporal separation and perpendicular baselines, it was possible to identify the area affected by ground deformation. Seasonal deformation signals were recognized at the southwestern part of the basin, reaching several centimeters during summer period.

1 Introduction

Land subsidence is a gradual settling or sudden sinking of the Earth's surface owing to subsurface movement of earth materials. The compaction of unconsolidated aquifer systems that can accompany excessive ground-water pumping is by far the single largest cause of subsidence. Land subsidence due to large amount of water withdrawal from an aquifer occurred in numerous regions throughout the world and is characterized, as a potential risk especially in the case the overlapping surface is a build up area. Subsidence is directly resulted from lowering of the piezometric surface due to fluid extraction. Poland and Davis (1996) demonstrated that the centers of subsidence coincided with the centers of major pumping. The magnitude and spatial extend of such vertical displacements are not easily detectable with conventional geological and geotechnical methods, which are additionally expensive and time consuming.

Interferometric Synthetic Aperture Radar (InSAR) technique has a great potential to detect and quantify ground subsidence caused by aquifer system compaction. A great number of researchers demonstrated the capability of Differential InSAR (DInSAR) to detect and measure ground subsidence, caused by the removal of subsurface groundwater (Galloway et al. 1998, Amelung et al. 1999, Fruneau et al. 2005, Parcharidis et al. 2006).

N. Lambrakis et al. (Eds.), *Advances in the Research of Aquatic Environment, Vol. 2*
DOI 10.1007/978-3-642-24076-8,

The aim of this study is to investigate surface deformation signals associated with annual precipitations and groundwater withdrawal, demonstrating the suitability of DInSAR for examining dewatering induced subsidence. Specifically, we attempt to measure seasonal deformation and its spatial distribution. Displacement maps of high spatial resolution were generated for the broader Larissa Plain using SAR acquisitions from ERS and ENVISAT satellites.

2 Larissa Plain

The present study is focused on the Southern part of Larissa plain, within the Thessaly basin, located in Central Greece (Fig. 1). Physiographically the area represents a typical plain of about 13700 km^2, surrounded by mountain ranges and traversed by Pinios River. The elevation ranges from sea level at the eastern coastal region to more than 2800 m at the eastern and western mountain areas, with mean elevation at nearly 500 m.

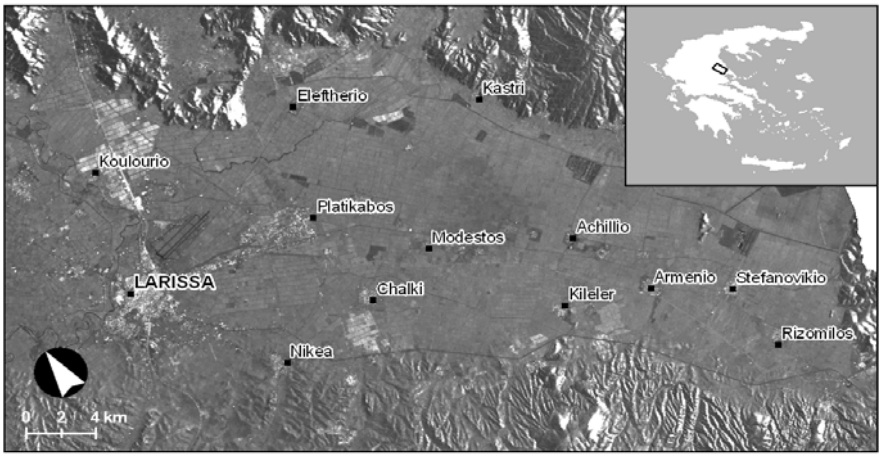

Fig. 1. Average intensity SAR image of Southern Larissa Plain.

During summer season in Thessaly is usually very hot and dry and in July and August temperatures can exceed 40°C. Mean annual accumulated precipitation varies from 400 mm at the plain area to more than 1850 mm at the western mountain ranges (Loukas and Vasiliades 2004). More specifically, the mean annual accumulated precipitation of the meteorological station at the airport of Larissa (22° 25′, 39° 38′) and it is operated from the Hellenic National Meteorological Service is 423,2 mm for a 43 year period (1955-1997). During this period the meteorological station which is located southeasterly of Larissa, near the city of Volos (22° 48′, 39° 13′), is recorded a slightly increased mean annual precipitation up to 500 mm.

The geomorphology of Thessaly is controlled by two orientations of normal faults. The main NW-SE trending basins of Karditsa and Larissa and their separating range are controlled by NW-SE trending normal faults (Caputo and Pavlides 1993). The younger normal faults strike E-W forming graben that cross-cut the older structures, uplifting and offsetting Late Quaternary deposits (Caputo 1993) and are concentrated in a northern and a southern zone. The northern zone at the north of Larissa basin comprises the Rodia, Tyrnavos and Larissa-Omolio faults (Caputo 1993). It is less active seismically in modern and historical times with just one earthquake of Ms 6.1 in 1941.

The bedrock geology consists of gneiss, schists, marbles, quartzites, serpentinites, flysch and carbonate formations (Paleozoic to Upper Cretaceous). The Quaternary sediments covering the basin consist of lacustrine and fluvial deposits poorly consolidated, with predominance of the fine grain size (Kaplanides and Fountoulis 1997). Very rich aquifers are observed in the poorly consolidated Quaternary formations and in the karstified carbonate rocks of the basin bedrock. The depth of water table varies considerably within the area.

Larissa Plain is characterized as the most cultivated and productive agricultural region in Greece. The extensive cultivation has lead to a remarkable increase of water demand, which is usually fulfilled by the over-exploitation of ground-water resources. Only a small part of this demand is covered by the Pinios River, its tributaries as well as a few small reservoirs and lagoons adjacent of Pinios River (Loukas and Mylopoulos 2004).

The above increased water demand has been associated with severe extreme and persistent droughts during the period from mid to late 1970s and the period from late 1980s to mid 1990s, interrupted by the wet 1990-1991, which mostly affected the northern part of Thessaly Basin (Loukas and Vasiliades 2004). These dry conditions result in irrigation cutbacks, overexploitation of groundwater and significant losses of crop yields. The subsidence phenomenon caused considerable damages to buildings in the area. Field observations made by the authors' indentified subsidence induced ground fissures in locations like Larissa-Airport, Kambos, Nikea and Melia villages.

3 SAR interferometric processing

The broader study area was repeatedly imaged by the European Space Agency satellites. For the purposes of this study, 48 ERS-1 and ERS-2 SAR scenes (Track 279 – Frame 2812 in descending mode) and 39 ENVISAT ASAR scenes (Track 279 – Frame 2807 in descending and Track 143 – Frame 783 in ascending modes) were acquired covering the periods 1992-2001 and 2001-2010 respectively. For the selection of the interferometric pairs (Table 1), we adopted two main criteria. First, a perpendicular baseline (Bp) component of up to 150 m was considered, although few pairs with slightly higher values were to be useful. Second, we dealt

on orbit pairs of different time spans and epochs in order to capture short and long term deformation signals.

Table 1. Interferometric parameters of the DInSAR pairs.

Sensor	Track	Dates	Total months	Bp (m)	Orbit
ERS	279	31/12/1995 – 14/04/1996	3.5	11.1	descending
ERS	279	02/08/1998 – 06/09/1998	1.2	-1.4	descending
ENVISAT	143	05/08/2004 – 09/09/2004	1.2	-23.3	ascending
ENVISAT	279	11/01/2009 – 15/02/2009	1.2	330.9	descending

The meteorological station at the airport of the city of Larissa accumulated 205.6 and 14.7 mm during the winter periods (31/12/1995 – 14/04/1996 and 11/01/2009 – 15/02/2009) and 0.4 and 18.5 mm during the summer periods referenced in the Figure 2.

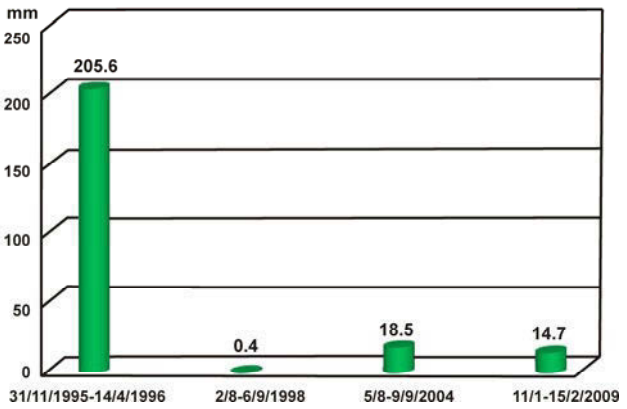

Fig. 2. Accumulated precipitation recorded by the Larissa meteorological station.

Interferometric processing was performed using GAMMA s/w packages (Wegmüller et al. 1998). Initial estimates of the interferometric baselines were calculated from available DORIS and DELFT precise orbit state vectors. A default number of 9 state vectors are initially given on 60s intervals. Due to the insufficient number of state vectors provided, in terms of cover of the area of interest, additional state vectors with an interval of 5.0s were introduced by respectively interpolation of the available state vectors and orbit propagation.

Precision co-registration based on the intensity cross correlation technique was implemented, achieving accuracies of sub-pixel level (~0.3 pixels). After removal of flat-Earth phases using the estimated interferometric geometry parameter values and refinement of the baselines, no phase ramps (orbital fringes) were recognized in the differential interferograms.

Topography related phases were simulated based on SRTM V3 DEM of approximate 90 m spatial resolution, oversampled to 20 m to fit with that of SAR data. Although the area exhibit rugged terrain, small perpendicular baselines ensures the minimization of possible topographic residuals. An adaptive filtering of the differential interferograms based on the local fringe spectrum was considered to assist and reduce possible residues during the unwrapping procedure. Unwrapping of differential phases was performed by applying a Minimum Cost Flow (MCF) algorithm (Costantini 1998).

Finally, accurate geocoding of interferometric results enables not only precise overlays with other data sources in a common map geometry, but also normalization for the systematic influence of terrain on image radiometry during image co-registration step. Finally a large number of interferograms were obtained, specifically 65 ERS pairs (Bp ≤50 m) and 48 ENVISAT pairs (Bp ≤150 m) in descending mode as well as 23 ERS pairs (Bp ≤100 m) and 43 ENVISAT pairs (Bp ≤400 m) in ascending mode.

4 Results and discussion

Interferometric pairs of short temporal separation and baselines were mainly utilized for the needs of the study, due to intensive decorrelation phenomena observed. Coherence levels are dramatically reduced within few months, narrowing the time span for robust observations.

It was possible however, to obtain an almost continuous displacement field and to delineate the area affected by ground deformation. Deformation patterns corresponding to ground subsidence are evident in interferograms covering the period between May and October. The deformed area (about 180 km^2) retains an elongated shape with NW-SE orientation (major axes almost 25 km), while covering only the southeastern part of the plain. The area of maximum deformation is located to the North of Kileler village, reaching -17.5 cm along the line of site in the summer of 1998 (from August to September), whereas for the same period in 2004 lower but also significant magnitudes of -12.7 cm are observed (Fig. 3). During winter seasons deformation is considerably reduced to -0.5 cm and -0.1 cm for 3.5 months (Dec.1995 – April 1996) and 1.2 months (Jan. – Feb. 2009) period respectively (Fig. 4). Rebound phenomena with significantly lower values were observed during high precipitation periods mainly at the NE of the basin (Fig. 3).

Larger subsidence should be expected when considering the entire summer season, where most of the irrigation and over-exploitation of ground-water are taking place. Accurate estimation of the deformation with conventional DInSAR techniques is however, not easily archived for larger time spans, due to extend of decorrelation phenomena in the region. Alternatively, it is questionable whether the implementation of advance processing techniques, such as Interferometric Stacking and PSInSAR, would offer better results. The magnitude and the pronounced

seasonal character of the deformation signal could not easily described adopting linear time-dependent models.

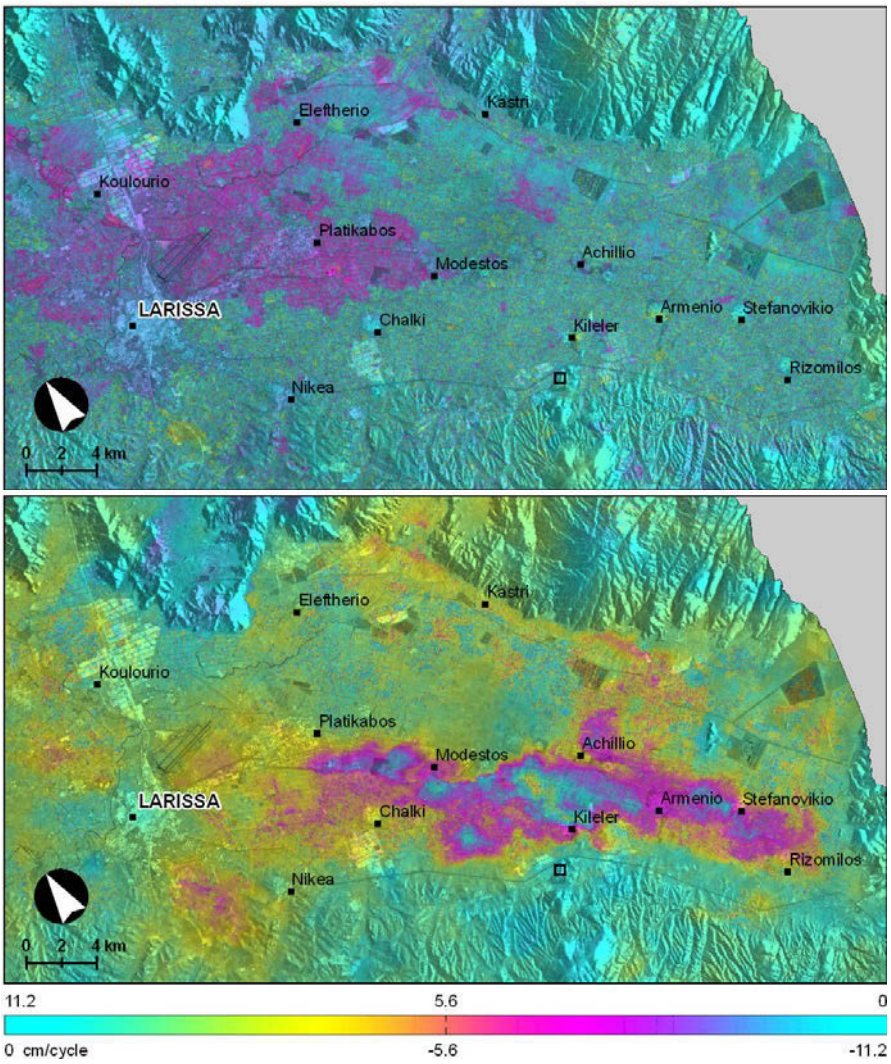

Fig. 3. Differential SAR interferograms between winter scenes 31/12/1995 – 14/04/1996 (up) and summer scenes 02/08/1998 – 06/09/1998 (down). Square corresponds to the reference point.

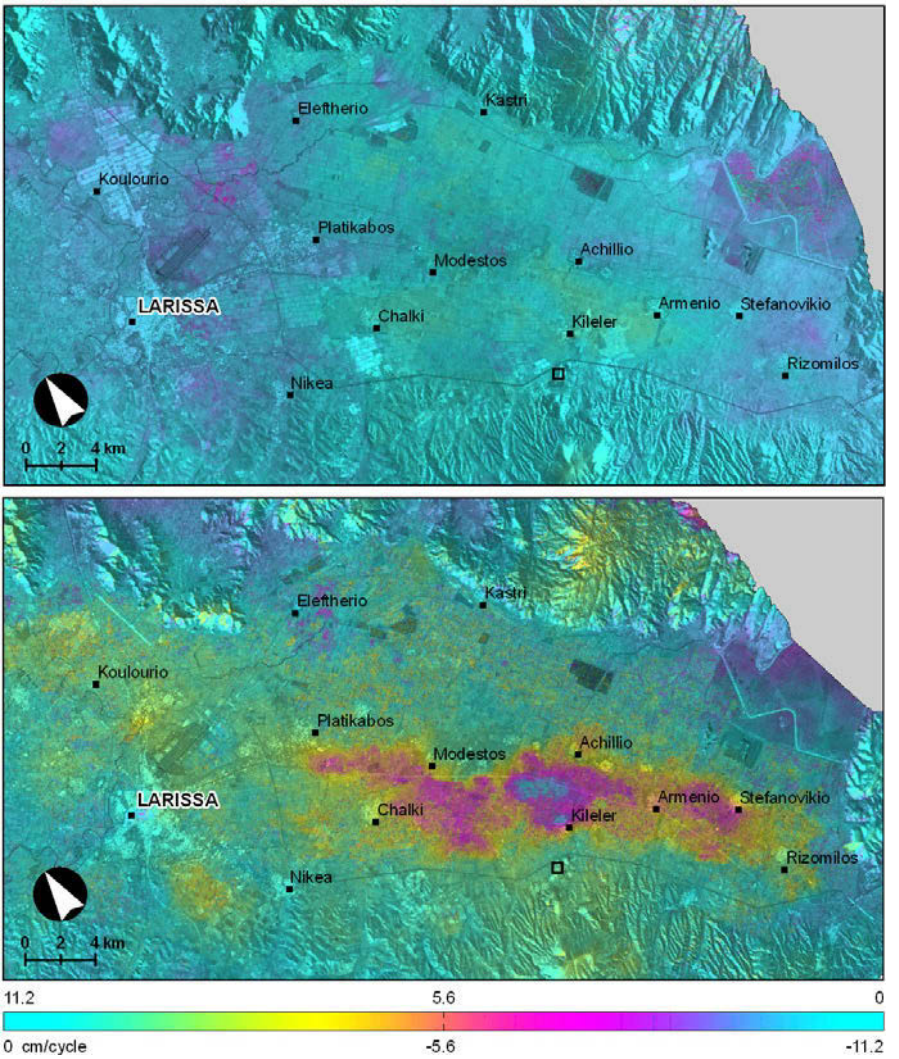

Fig. 4. Differential SAR interferograms between winter scenes 11/01/2009 – 15/02/2009 (up) and summer scenes 05/08/2004 – 09/09/2004 (down). Square corresponds to the reference point.

Acknowledgments The present study is part of TERRAFIRMA_X project supported by ESA's GMES Service Element Program. ERS SAR and ENVISAT ASAR scenes were provided by ESA within the frame of the project.

References

Amelung F, Galloway DL, Bell JW, Zebker HA, Laczniak RJ (1999) Sensing the ups and downs of Las Vegas: InSAR reveals structural control of land subsidence and aquifer-system deformation. Geology 27, 483–486

Caputo R, Pavlides S (1993) Late Cenozoic geodynamic evolution of Thessaly and surroundings (central-northern Greece). Tectonophysics 223 (3-4), 339-362

Caputo R (1993) Morphotectonics and kinematics of the Tyrnavos fault, northern Larissa Plain. Zeitschrift fur Geomorphologie 94, 167-185

Costantini M (1998) A novel phase unwrapping method based on network programming. IEEE Transactions on Geoscience and Remote Sensing 36 (3), 813-821

Fruneau B, Deffontaines B, Prunier-Leparmentier A.-M, Arnaud, A (2005) Reflexions and insights from Urban SAR interferometry for monitoring vertical deformation due to water pumping: The Haussmann-St-lazare case example (Paris, France). European Space Agency, (Special Publication) ESA SP (572), art. no. 575, 947-951

Galloway DL, Hudnut KW, Ingebritsen SE, Phillips SP, Peltzer G, Rogez F, Rosen P (1998) Detection of aquifer system compaction and land subsidence using interferometric synthetic aperture radar, Antelope Valley, Mojave Desert, California. Water Resources 34, 2573–2585

Kaplanidis A, Fountoulis D (1997) Subsidence phenomena and ground fissures in Larissa, Karla Basin, Greece: Their results in urban and rural environment. In: Proc. of the International Symposium “Engineering Geology and the Environment” v.1, 729-735

Loucas A, Mylopoulos M (2004) Effects of hydrotechnical works development and water resources management on the availability of water resources of Pinios river basin. In: Proc. of the 7th International Conference of Protection and Restoration of the Environment. Mykonos

Loukas A, Vasiliades L (2004) Probabilistic analysis of drought spatiotemporal characteristics in Tessaly region, Greece. Natural hazards and Earth System Sciences 4 (5-6), 719-731

Parcharidis I, Lagios E, Sakkas V, Raucoules D, Feurer D, Le Mouelic S, King C, Carnec C, Novali F, Ferretti A, Capes R, Cooksley G (2006) Subsidence monitoring within the Athens basin (Greece) using space radar interferometric techniques. Earth Planets and Space 58, 505-513

Poland JF, Davis GH (1996) Land subsidence due to withdrawal of fluids. In: Varnes DJ (ed) Reviews in engineering geology v.II, 187-268. Geological Society of America, Boulder Colorado

Wegmüller U, Werner C, Strozzi T (1998) SAR interferometric and SAR differential interferometric processing chain. In: Proc. of IGARSS v.2 pp. 1106-1008